Ultraenergetic Heavy-Ion Beams in the CERN Accelerator Complex for Radiation Effects Testing

Rubén García Alía, Pablo Fernández Martínez, Maria Kastriotou, Markus Brugger, Johannes Bernhard, Matteo Cecchetto, Francesco Cerutti, Nikolaos Charitonidis, Salvatore Danzeca, Lau Gatignon, Alexander Gerbershagen, Simone Gilardoni, Nourdine Kerboub, Maris Tali, Vanessa Wyrwoll, Véronique Ferlet-Cavrois, César Boatella Polo, Hugh Evans, Gianluca Furano, and Rémi Gaillard

***Abstract*— Traditional heavy-ion testing for single-event effects is carried out in cyclotron facilities with energies around 10 MeV/n. Despite their capability of providing a broad range of linear energy transfer (LET) values, the main limitations are related to the need of testing in a vacuum and with the sensitive region of the components accessible to the low range ions. In this paper, we explore the use of ultrahigh energy (UHE) (5–150 GeV/n) ions in the CERN accelerator complex for radiation effects on electronics testing. At these energies, we show, both through simulations and experimental data, the significant impact of the ion energy on the ionization track structure and associated volume-restricted LET value, highlighting the possible limitations for radiation hardness assurance for high-energy accelerator applications. In addition, we show that from a nuclear interaction perspective, UHE ions behave similar to protons independently of their significantly larger mass.**

***Index Terms*— FLUKA , CERN, Monte Carlo simulation, single event effects (SEEs).**

I. Introduction

TRADITIONAL heavy-ion (HI) tests for single-event effect (SEE) qualification are carried out in cyclotron facilities with energies around 10 MeV/n. The figure-of-merit for the tests is the linear energy transfer (LET), which for energies in standard facilities can be varied over a large interval (typically 1–60 MeVcm^2/mg) by changing the ion species and when possible energy. Moreover, for cases in which the dependence of the deposited energy with the incidence angle is known, this parameter can be used to further increase the effective LET for a given ion and energy. The combination of different ion beam parameters allows to obtain the SEE cross section as a function of LET, which can then be folded with the environmental LET curve [typically that of galactic cosmic rays (GCR)] in order to obtain the expected SEE rate [1]. Even if the vast majority of ions in the GCR spectra, peaking in the 500-MeV/n–1 GeV/n range, are above the energies used in standard HI facilities, the representation of the environment through its LET spectra enables the application of the ground test data to estimate the in-orbit SEE rate.

For high-energy accelerator applications [2], SEE qualification is typically carried out using 200-MeV protons and/or a mixed-field environment such as that available in the Cern High-energy AcceleratoR Mixed-field (CHARM) facility [3]. Such test conditions are representative of the SEE effects in the accelerator environment [4] dominated by indirect energy deposition from high-energy (>20 MeV) hadrons (HEH, mainly pions, neutrons, and protons). However, SEE testing with ions of an LET large enough to exclude indirect energy-deposition SEEs from HEH is sometimes performed for critical components and failure modes (e.g., destructive SEEs) due to the reduced associated beam time and total ionizing dose (TID) levels.

Ions with energies of 10 MeV/n typically used in standard facilities (e.g., RADEF [5], [6]) have ranges in silicon from 70 μm for xenon, up to 270 μm for carbon. Therefore, parts need to be delidded in order to make their sensitive volumes (SVs) accessible to the beam, and tests need to be carried out in vacuum to avoid that the ions range out in air. However, state-of-the-art complex parts are often too difficult or costly to delid, or have SVs inaccessible for standard energy HIs [7]. Similarly, 3-D stacked structures (e.g., system in package) are becoming ever more popular thanks to the reduced wire delay and increased IC density. Moreover, even if the SV is reached, in order for the SEE results as a function of LET to be meaningful, the range needs to be sufficient to cover the full SV thickness with a roughly constant LET value. As has been shown in the past, ions with similar LETs but different ranges can lead to very different SEE responses [8] due to insufficient beam penetration. Therefore, testing at larger ion energies can be beneficial both in terms of not requiring part opening and testing in a vacuum, as well as for guaranteeing a constant LET throughout the entire sensitive thickness.

Manuscript received September 15, 2018; revised October 25, 2018 and November 21, 2018; accepted November 21, 2018. Date of publication November 28, 2018; date of current version January 17, 2019.

R. G. Alía, P. F. Martínez, M. Kastriotou, M. Brugger, J. Bernhard, M. Cecchetto, F. Cerutti, N. Charitonidis, S. Danzeca, L. Gatignon, A. Gerbershagen, S. Gilardoni, N. Kerboub, M. Tali, and V. Wyrwoll are with CERN, 1211 Geneva, Switzerland (e-mail: ruben.garcia.alia@cern.ch).

V. Ferlet-Cavrois, C. Boatella Polo, H. Evans, and G. Furano are with European Space Agency, ESTEC, 2200 AG Noordwijk, The Netherlands.

R. Gaillard resides in 78730 Saint-Arnoult, France.

Color versions of one or more of the figures in this paper are available online at http://ieeexplore.ieee.org.

Digital Object Identifier 10.1109/TNS.2018.2883501

TABLE I
HI ENERGY RANGES AS CONSIDERED IN THIS PAPER

Standard Energy (SE)	$<$ 10 MeV/n
High Energy (HE)	10-100 MeV/n
Very-High Energy (VHE)	100 MeV/n-5 GeV/n
Ultra-High Energy (UHE)	5-150 GeV/n

In order to differentiate between the various energy ranges and respective facilities, we here define standard energies (SEs) as those up to 10 MeV/n, such as in the UCL [9] and RADEF [10] facilities. High energies (HEs) are considered as the 10–100-MeV/n interval, and are obtainable in facilities such as TAMU [11], BASE [12], GANIL [13], or KVI [14]. We regard very HEs (VHEs) as those in the 100-MeV/n–5 GeV/n range, available for instance at GSI or NSRL [15]. Finally, ultra-HEs (UHEs) are defined as ions in the 5–150-GeV/n range, such as those available in the CERN accelerator complex, and which are the main subjects of this paper. The defined energy intervals are summarized in Table I. SEE tests in the UHE regime were previously performed in the alternating gradient synchrotron (AGS) at Brookhaven National Laboratory [16], sister machine of CERN's proton synchrotron (PS). Whereas the AGS SEE experiments were performed with a gold beam at 11.4 GeV/n, the ion energy in the beam described in this paper can reach 150 GeV/n.

As will be detailed later on, the VHE and UHE HI beams can be used to: 1) evaluate system-level soft errors and 2) screen parts for destructive effects up to a certain LET value. This paper mainly focuses on the second point for screening of components and subsystems for hard failures in the HE accelerator environment, for which as will be covered in detail, the main identified limitation is the relatively low LET value associated with the UHE ion beams.

However, in order to efficiently apply UHE HI beams to the evaluation of board-/system-level soft errors and hard SEE failure screening, their physical interaction with the components needs to be carefully understood. The very different energy regime with respect to SE and HE HI testing implies also potentially very distinct interaction characteristics and thus repercussion on the qualification result. Therefore, this paper focuses on three fundamental aspects related to the impact of the UHE beam on the potential SEE induction: 1) the LET restricted to micrometric volumes representative of the SEE sensitive regions; 2) the evolution of the beam characteristics in its passage through matter (e.g., different test boards placed sequentially in the beam); and 3) the impact of indirect energy deposition through nuclear reaction products. The assessment will mainly be carried out by means of Monte Carlo simulations using the `FLUKA` Monte Carlo tool [17], [18], but will also include an initial experimental evaluation. This paper will also focus on the associated radiation hardness assurance (RHA) implications.

This paper is structured as follows. The UHE HI beams in the CERN accelerator complex are presented in Section II, and the analysis of their interaction with matter in the scope of SEE induction is described through Monte Carlo simulations in Section III. Experimental results from the 2017 UHE HI test campaign are described in Section IV, and the possible RHA applications for the accelerator mixed-field environment are included in Section V. Finally, Section VI features the conclusions and outlook of this paper.

II. UHE HEAVY-ION BEAMS IN THE CERN ACCELERATOR COMPLEX

The CERN accelerator complex is a versatile injection and collider chain capable of accelerating both protons and HIs. However, proton physics constitutes the core program of CERN's most energetic accelerator, the large hadron collider (LHC); HIs are also accelerated to produce tera electron volt-energy collisions in the LHC experiments, notably in a large ion collider experiment, a detector specifically tailored for ion physics. A schematic of the CERN accelerator complex can be seen in [19], where the main area of interest for this paper is the north area (NA), receiving beam from the super PS (SPS) ring through the TT20 line.

One previous step in the injector chain, the CHARM facility is shown as extracted from the PS. The facility is typically operated by interacting the 24-GeV/c proton beam from the SPS with a 50-cm copper target [3], however testing components and boards directly with the UHE proton beam is also possible [20]. It is worth noting that during 2017 ion operation and in addition to the NA experiments described in this paper, an ion beam was used for the first time for radiation effects testing in the IRRAD/CHARM areas. The associated beam conditions and experimental results are covered in [21].

Related to their availability for the LHC physics program, HIs are also used in the LHC injectors for fixed-target experiments [22]. Ions in the SPS are fully stripped and can be extracted to the NA with a momentum in the 30–400-ZGeV/c range, corresponding to 13–150 AGeV/c. The spill duration for the NA depends on the overall optimization for the SPS and its users, and can be between 4.5 and 10 s. The flat-top slow extraction is theoretically of uniform intensity.

Spills are received with a periodicity of $\sim$48 s. The extracted beam from the SPS is transported over about 1 km by bending and focusing magnets and then split into three branches, directed toward three primary target stations: T2, T4, and T6. Ion beams can either be fragmented, when interacting with the targets, or primary beams, as those used in this paper is described here. As will be further detailed in Section IV, the beam line used for the results presented in this paper is the H8 beam line, derived from the T4 target in the SPS NA.

The ion program in the CERN injector chain is typically scheduled during roughly 4 weeks at the end of the annual runs (November–December) and is dedicated to a single-ion species, generally lead. The experiments described in this paper were carried out during the 2017 xenon run. Further radiation effects on electronics campaigns are scheduled for the 2018 lead run, for which 120 h of beam time have been allocated. After 2018, the 2 year long shut down 2 (LS2) will interrupt the irradiation activities linked to the LHC and its injector chain until 2021.

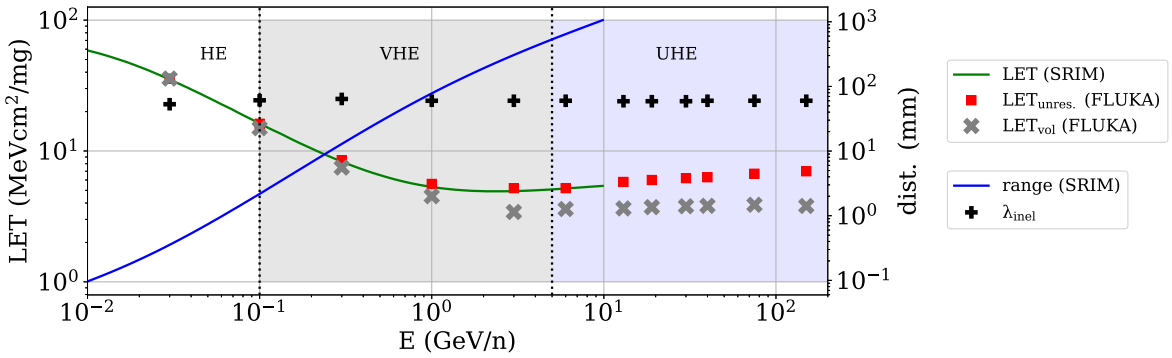

Fig. 1. Unrestricted and volume-equivalent (1 μm^3) LET for a xenon beam in the energy range covering from SE to UHE. The range and inelastic interaction length λ are also shown in a different axis.

III. Interaction of UHE Heavy-Ion Beams for Radiation Effects on Electronics

A. Direct Ionization and Volume-Equivalent LET

In their passage through matter, charged particles such as HIs will produce secondary electrons through ionization. If such secondary electrons are themselves capable of producing further ionization, they are referred to as delta rays. For SE ions of 10-MeV/n energy and according to the Hutcheon equation [26], the maximum kinetic energy transferred to a delta ray is 22 keV, which corresponds to a range of roughly 6 μm in silicon, meaning that a very large fraction of the energy lost by the ion will be deposited locally in a micrometric radial track. However, ions with larger energy will, in turn, transfer higher energies to the delta rays, and therefore, a significant fraction of the lost energy can be deposited outside the micrometric vicinity of the ion trajectory.

In order to evaluate the impact of the ionization track structure on the capability of inducing SEEs, we consider a generalized cubic SV of 1 μm^3 in a surrounding silicon material of a larger, 10-μm side cube. The deposited energy through direct ionization is scored on an event-by-event basis with FLUKA, using the lowest permissible delta-ray threshold of 1 keV. Calculations presented in this paper were performed using FLUKA2011 Version 2x.2. The resulting average energy-deposition distribution is divided by the SV thickness of 1 μm in order to obtain the volume-equivalent LET and compare it to the total (unrestricted) value. Of course, through this definition, the volume-equivalent LET will depend on the considered SV and surrounding dimensions, as well as on the physical settings of the Monte Carlo simulation, notably the delta-ray threshold, which should be selected according to the considered SV size in order to optimize the simulation's CPU efficiency.

The concept of volume-equivalent LET has been previously introduced in different contexts, such as that of retrieving a more accurate in-flight SEE rate from the GCR spectrum [23] or that of linking the proton and HI sensitivity [24], [25].

The results of the simulated volume-equivalent LET values are shown in Fig. 1 for xenon in the energy range covering from SE to UHE, together with the tabulated unrestricted value as extracted using SRIM [27] up to 10 GeV/n and FLUKA for energies above. The range and inelastic interaction length λ are also shown and will be further discussed in Sections III-B and III-C.

As can be seen, whereas the volume-equivalent LET for xenon matches the unrestricted value for energies up to roughly 300 MeV/n, the two quantities diverge above this value, and in the UHE range, the volume-equivalent LET is only 50%–55% of the unrestricted value. This implies that: 1) for destructive SEEs, the volume-equivalent LET value needs to be taken into account when applying the results to other environments such as the HE accelerator mixed field and 2) because of the very high delta-ray energies and large radial dimensions, multiple cell upsets (MCUs) could be produced in a significantly larger proportion than at lower energies [28]. MCUs are relevant as they can lead to multiple-bit upsets (i.e., multiple upsets in the same logical word) which cannot be corrected by standard error correction codes. This last point is not directly treated in this paper but could be a subject of further research.

The numerical volume-restricted LET values plotted in Fig. 1 are shown numerically in Table II for the ion energies available in the CHARM PS East Area (6 GeV/n) and SPS NA (13–150 GeV/n). The ions considered are xenon and lead as part of the CERN injector ion physics program, and uranium as available in the VHE regime at GSI. At NSRL, the very similar thorium ion is available.

As a complementary view of the differences between the unrestricted and volume-restricted LET values shown in Fig. 1, the radial profiles of the ionization track of a 9.3-MeV/n Si ion (LET = 6.40 MeVcm^2/mg according to SRIM) and a 40-GeV/n Xe ion (LET = 6.3 MeVcm^2/mg according to the tabulated FLUKA value) are scored cylindrically in FLUKA in a 1-μm-thick slab, 5 μm after having entered the silicon material. The results are shown in Fig. 2. Whereas the radial distribution of the Si SE ion falls off rapidly above 5 μm, that of the UHE Xe beam with a similar LET extends up to the end of the scoring region, set at a radius of 100 μm. By integrating the deposited energy up to a certain radius and dividing it by the scoring region thickness, the LET restricted to that volume can be obtained. If this is done for a radius of 1 μm in the case of the Si ion, the unrestricted LET value is recovered, manifesting that the vast majority of energy is deposited within the associated column. However, in the case of Xe, the LET restricted to a 1-μm radius is 3.6 MeVcm^2/mg,

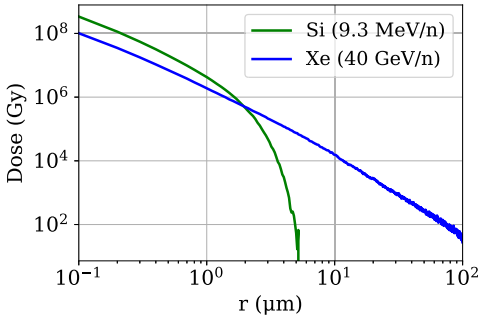

Fig. 2. Radial distribution of pencil ion beams on a 100-μm radius silicon cylinder at a depth of 5 μm and scoring thickness of 1 μm. Despite the very different energy and Z, both ions have a very similar unrestricted LET value of 6.3–6.4 MeVcm^2/mg.

TABLE II

VOLUME-EQUIVALENT LET IN UNITS OF MeVcm^2/mg FOR DIFFERENT UHE IONS AS SIMULATED IN FLUKA FOR AN SV OF 1 μm^3. IN ALL CASES, THE ASSOCIATED 1-SIGMA STATISTICAL UNCERTAINTY IS BELOW 2%. THE TABULATED UNRESTRICTED LET VALUES, ALSO TAKEN FROM FLUKA, ARE SHOWN IN BRACKETS

Energy (GeV/n)	Ion		
	Xe	Pb	U
6	3.60 (5.0)	7.98 (11.7)	9.83 (14.7)
13	3.64 (5.8)	8.33 (12.6)	10.32 (15.8)
19	3.72 (6.0)	8.63 (13.0)	10.39 (16.4)
30	3.78 (6.2)	8.41 (13.6)	10.56 (17.1)
40	3.71 (6.3)	8.45 (13.9)	10.47 (17.5)
75	3.88 (6.7)	8.80 (14.6)	10.99 (18.4)
150	3.80 (7.0)	8.80 (15.3)	10.82 (19.3)

i.e., only a fraction of the total value, compatible with that shown in Table II. In addition to the reduced effective LET in the central part of the ionization column, possible effects such as enhanced MCU induction could be associated with UHE ions, especially in the case of technologies directly sensitive to delta rays [29].

The simulated effects of the UHE ionizing track structure and related volume-equivalent LET values will be compared with experimental single event upset (SEU) results in Section IV and used to derive the related RHA implications in Section V.

B. Nuclear Reaction Impact on Indirect Energy-Deposition SEEs

Nuclear interactions, while being the main source of proton- and neutron-induced SEEs through indirect energy deposition, are typically not considered in SE HI tests due to the dominance of direct ionization and the relatively small probability of a nuclear interaction occurring before the ion ranges out. However, in the UHE regime, with lower LET values and much larger ranges, nuclear reactions are expected to play a more important role.

The probability of a particle interacting through a nuclear reaction after having traveled a distance x in a certain material is given by (1), where λ is the inelastic interaction length, σ is the nuclear reaction cross section, and N is the material nuclear density, related to Avogadro's number N_A, the atomic number A, and the material density ρ through (2). Therefore, the relationship between the inelastic interaction length (in centimeters) and the reaction cross section in silicon (in millibarns, or 10^{-27} cm^2) can be expressed as shown in (3). As shown in Fig. 1, the inelastic interaction length for UHE xenon beams in silicon is roughly 6 cm, corresponding to a reaction cross section of 3300 mb. For 200-MeV protons typically used for space and accelerator qualification, the associated interaction length and nuclear reaction cross section in silicon are, respectively, 49.7 cm and 402 mb. Therefore, for a given small thickness with respect to λ, a xenon UHE beam has a probability of interacting with silicon a factor ~8 larger than protons typically used for SEE qualification.

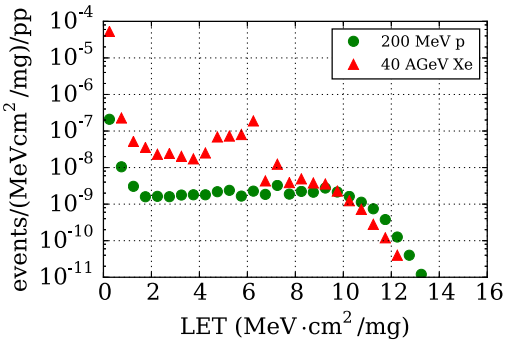

Fig. 3. LET distribution of nuclear silicon fragments for different beams.

In the UHE regime (5–150 GeV/n), the inelastic interaction length for Xe in silicon is largely independent of the ion energy and can be considered to be 6.0 cm. For the other two heavier ions studied in this paper, Pb and U, the value is, respectively, 4.9 and 4.7 cm, therefore weakly depending on the Z of the projectile ion

$$P_{\text{int}}(x) = 1 - e^{-\frac{x}{\lambda}} = 1 - e^{-N\cdot\sigma\cdot x} \tag{1}$$

$$N = \frac{N_A}{A}\cdot\rho \tag{2}$$

$$\lambda_{\text{Si}}(\text{cm}) = \frac{2.00\cdot 10^4}{\sigma_{\text{Si}}(\text{mb})}. \tag{3}$$

In addition to the total probability, the nature of the fragments produced in the nuclear reactions is also highly relevant for evaluating their possible impact on indirect energy deposition and SEE induction. In order to study this distribution, FLUKA was used to score the LET of the nuclear reaction products created by the 40-GeV/n xenon beam with a silicon micrometric target. Above 5 GeV/n, an adaptation of the DPMJET code [30] is used as nucleus–nucleus event generator, with the evaporation stage of excited residual nuclei fully performed in FLUKA.

As shown in Fig. 3, the LET distribution of the secondaries is very similar to that produced by 200-MeV protons in silicon, the main difference between the two arising near the LET of the projectile and lower values, which therefore account for most of the nuclear reaction cross section difference. Therefore, a component with an LET threshold above that of the primary beam is expected to have a similar SEE cross section to that associated with HE protons, in agreement to

TABLE III
RELATIVE BEAM INTENSITY AS A FUNCTION OF DISTANCE IN SILICON, BOTH AS CALCULATED IN FLUKA AND AS EXTRACTED ANALYTICALLY FROM (1)

Distance in Si (mm)	Relative Intensity	
	FLUKA	Analytic
1	0.98	0.98
2	0.97	0.97
3	0.95	0.95
5	0.92	0.92
10	0.86	0.85
20	0.73	0.72
30	0.63	0.61
50	0.46	0.43

what was observed experimentally and through simulation in [8] and [31]. Thus, it can be concluded that reactions in the VHE and UHE regimes have cross sections that only weakly depend on the ion mass and are therefore comparable to those associated with protons and neutrons.

This situation is very different from nuclear reactions in the SE HI range, in which complete or break-up fusion can take place between the projectile and target nuclei, generating mass and LET values significantly larger than those associated with the original projectile and target separately [32].

Moreover, whereas this paper focuses on ion fragments in silicon, it has previously been shown that, similar to protons, energetic HIs are capable of producing large LET fission fragments (up to $\sim$40 MeVcm^2/mg) when interacting with high-Z materials near the SV such as tungsten [32], [33].

C. Beam Property Evolution in Its Passage Through Matter

As expected by the very large range and constant LET values of the UHE beams shown in Fig. 1, as well as the relatively low high-LET fragment production yield presented in Fig. 3, the changes in the considered UHE xenon beam in its passage through matter are not related to energy loss through ionization and associated LET change or the production of fragments with larger LET than the beam itself, but rather to the intensity decrease due to nuclear reactions. In order to quantify this effect, FLUKA was used to score the LET distribution of the 40-GeV/n xenon beam in its passage through silicon. The relative intensity of beam particles with an LET of $\pm$2.5% of its initial value is shown in Table III for different silicon thicknesses, also including the expected analytic value according to (1).

Therefore, when testing multiple boards with equivalent silicon thicknesses of above $\sim$5 mm, it is necessary to take into account the beam attenuation due to nuclear reactions, either through Monte Carlo simulations in cases where an accurate description of the materials and thicknesses is available, or through measurements with, e.g., calibrated SEU monitors.

In addition, the fact that the beam intensity will significantly attenuate via nuclear reactions before changing its LET through ionization loss also implies that the UHE beams cannot be degraded to lower energies and larger LETs, as done for instance with the HE and VHE beams in KVI [31] and NSRL [7].

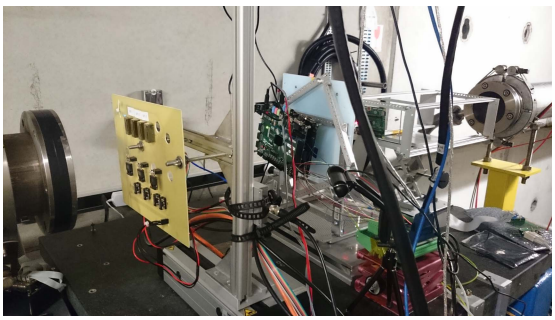

Fig. 4. Experimental setup in the SPS NA during the 2017 UHE xenon run. The beam travels left to right, and tests are performed in air with different boards tested sequentially after another.

IV. 2017 UHE ION RADIATION TEST CAMPAIGN IN THE H8 SPS NA BEAM LINE

During the 2017 xenon ion operation at CERN, electronics irradiation tests were carried out in the H8 beam line in November, using xenon beams of 19, 30, 40, and 75 AGeV/c. In addition to the calibration and experiments performed by the radiation to electronics (R2E) team at CERN with the support of the beam line and beam instrumentation physicists, a 1 week external user test campaign coordinated by CERN and the European Space Agency (ESA) took place, involving a broad range of components including SiC diodes and MOSFETs and state-of-the-art field-programmable gate arrays, often tested in parallel profiting from the high beam penetration, as shown in Fig. 4.

As introduced in Section II, the H8 secondary beam line in the SPS NA derives from target T4, which in the case of the experimental test campaign presented in this paper, was not intercepting the beam, enabling the use of the primary xenon beam with the SPS momentum. The positions of different beam line elements in H8 are expressed in terms of the distance z to the T4 location.

The beam intensity was monitored with a scintillator located at $z = 475$ m, also equipped with a signal splitter for pulse height analysis (PHA). The PHA was used to determine the fraction of scintillator counts corresponding to the primary beam, which roughly equated to 40% of the total counts. The remaining counts were attributed to minimum ionizing particles (i.e., protons, pions, and muons) propagated with the beam, and neglected for the SEE analysis due to their very low LET value with respect to the primary beam. The beam size was monitored with a horizontal ($z = 475$ m) and vertical ($z = 476$ m) multiwire proportional chambers. This instrument was used to measure the evolution of the beam profile with time, and at the test location ($z = 430$ m), radiochromic films were used additionally to measure the size relevant to the device under test (DUT) fluence calculation.

The spill intensity could be varied between roughly 10^2 and 10^6 ions per spill by means of two collimators located significantly upstream of the DUT location, with positions up

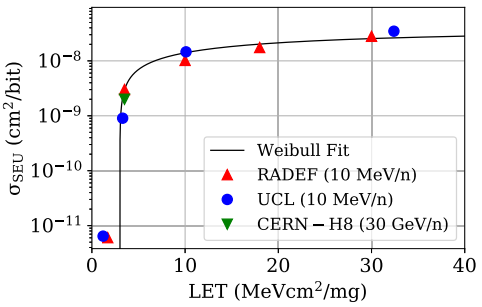

Fig. 5. SEU cross section as measured with the ESA SEU reference monitor in different HI facilities, including the UHE xenon beam at CERN.

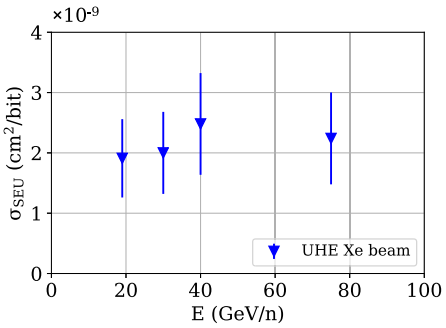

Fig. 6. SEU cross section for the ESA reference monitor and different UHE xenon energies tested in the CERN NA.

to $z = 203$ m. The collimators used to regulate the beam intensity did not impact the beam profile at the DUT position. The beam size depended on the specific beam optics, which was adjusted according to the irradiation requirements in an interval of 25–80-mm full-width half-maximum. The total spill duration was 8 s with a spill periodicity depending on the specific SPS operation but ranging from 30 to 50 s. Such settings resulted in average fluxes ranging from 1 ion/cm^2/s to 2×10^3 ions/cm^2/s. Despite the theoretical uniform beam intensity during the spills, a 50-Hz structure related to the SPS power converters was identified in the scintillator time-profile readout.

The ESA SEU standard monitor [34]–[36] was placed in the UHE xenon beam in H8 in order to, first of all, validate the beam alignment and its homogeneity over the 20×20 mm^2 sensitive surface. In addition, it was used to confirm the independence of the SEU cross section for a given beam energy and optics, and throughout the broad range of intensities used. The derived SEU cross section is shown in Fig. 5 together with the component's calibration in SE facilities and corresponding fit to a Weibull function. The LET considered for the H8 beam is the volume-equivalent value, as further described in Section III-A. As can be seen, the UHE SEU cross section result is compatible with similar LET values at SE facilities, however, it is to be noted that the considered LET region is very close to the threshold value; therefore, a large variability in the cross section is expected for small changes in the LET. Provided the equivalent-LET is defined through the energy deposited in a certain volume divided by its thickness, the main uncertainty associated with its calculation is related to the consideration of its dimensions.

Measurements were performed with the ESA SEU reference monitors for all energies tested (19, 30, 40, and 75 GeV/n) and at different moments in time, focusing on the changes of the experimental setup, involving a realignment of the equipment without a dedicated mechanical system. Therefore, one of the purposes of the reference SEU measurements was that of ensuring an adequate alignment and homogeneity of the beam. Such multiple measurements (typically 5–10 per energy) also enabled the calculation of the standard deviation between the measurements, accounting for the statistical spread related to the realignment of the equipment as well as in the applicable cases, the changes in the beam profile through the associated optics. The relative 2σ spread of different runs for the same energy was near but below 30%. This value is therefore considered as the uncertainty related to the single measurement alignment as well as to the beam size. The latter was only measured directly at the DUT location in selected runs through the radiochromic film, and otherwise relied on the correlation with the online, logged profile measurement with the instruments 45-m downstream of the DUT position.

In addition to this 30% uncertainty related to the beam alignment and profile, an additional 15% is considered associated with the beam intensity value measured through the scintillator counts and relative xenon contribution. Therefore, the total relative 2σ uncertainly for the ion fluences and associated SEE cross section measurements is considered to be ±34%, thus significantly above typical values for standard facilities (± ∼ 10%) but still precise enough to extract relevant conclusions with regards to the behavior of the UHE in terms of radiation-matter interaction for SEE induction.

The resulting SEU cross section for the reference monitor and different energies considered are shown in Fig. 6 together with the associated uncertainty. The main conclusions from these results are: 1) the satisfactory agreement between the UHE results and the SEU cross section value expected from the SE HI data set and 2) the very weak dependence of the UHE SEU cross section with energy, as expected from the very small variation in the volume-equivalent LET.

V. Possible Radiation Hardness Assurance Applications

Depending on their total number and associated radiation environment, semiconductor devices to be integrated in critical LHC systems need to be qualified up to proton or HEH ($E >$ 20 MeV) fluences reaching $\sim 10^{14}$ cm^{-2} [2], [4], [37]. This is typically carried out in proton test facilities such as the proton irradiation facility (PIF) in the Paul Scherrer Institute (PSI) [38], or the CHARM facility at CERN. Challenges related to achieving such fluence values include the associated beam time, the TID delivered to the parts, or the board activation. It is to be noted that such target proton fluence levels are three orders of magnitude above the 10^{11} p/cm^2 value specified for space standards (e.g., ESCC 25100).

All such aspects would benefit from a qualification approach with an HI beam of an LET large enough to exclude SEE in the HE accelerator mixed field (i.e., ∼15 MeVcm^2/mg when considering silicon) and an energy large enough to

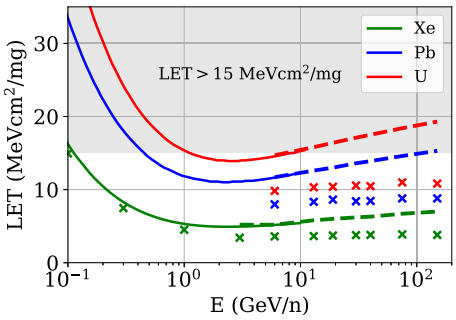

Fig. 7. Unrestricted (solid lines: SRIM, dashed lines: FLUKA) and volume-equivalent (crosses) LET values in the VHE and UHE regimes.

test multiple parts in air and in parallel without the need of opening and/or thinning. In order to evaluate such capability, Fig. 7 shows, for different ion calculations, the unrestricted and volume-equivalent LET values, as introduced in Section III-A. As can be seen, whereas in the UHE regime, the Pb beam would reach, at the HE end (150 GeV/n), an unrestricted LET value large enough to exclude SEEs in a mixed-field HE accelerator environment, the volume-equivalent LET value relevant for electronics testing is clearly below the limit, even for the case of the heavier U ion.

Therefore, despite the promising conditions associated with UHE ion testing, combining the advantageous aspects related to proton/mixed-field (high penetration) and HI (low target fluence and, therefore, reduced beam time, TID, and board activation) qualification; the associated volume-equivalent LET is not large enough to exclude SEE sensitivity for HE accelerator applications. An analogous argument would apply to qualification for the trapped proton space environment.

A possible alternative approach could be to profit from the very large beam penetration to tilt the angle of incidence on the component, potentially up to values near 90°, which for effects such as single-event latchup could result in an effective LET large enough to exclude indirect energy-deposition SEEs for accelerator applications. However, such an approach strongly depends on the topology of the associated SV and needs to be investigated in further detail.

VI. Conclusion

This paper describes the UHE ion beams at CERN and their possible application to SEE qualification. Because of the very different energy range to that typically employed in standard HI tests, the beam–matter interactions are analyzed in the context of radiation effects and with the aid of Monte Carlo simulation tools. Through this analysis, we show that in the VHE and UHE regimes, the volume-equivalent LET for typical SEE SV dimensions can be significantly lower than the unrestricted value, and therefore needs to be carefully considered when applying UHE results to other operational environments, such as the accelerator mixed field. In addition, we evaluate the impact of nuclear interaction of the beam with the component material, showing that they are the main source of the beam property evolution in its passage through matter resulting in its progressive intensity reduction. Moreover, it is shown that indirect energy-deposition events—and therefore sub-LET threshold SEE cross sections—are expected to be similar to those associated with HE protons.

With the considerations earlier, the UHE ion beams are regarded as a potentially interesting means of testing SEE components, mainly related to the high accessibility of the SV and the possibility of parallelizing multiple tests. In particular, the main interest for HE accelerator applications is that of using an UHE beam with a large enough LET to validate the immunity of components to hard failures in the mixed-field environment, otherwise requiring very large target proton or HEH fluence values related to the large radiation level and the number of system units distributed in the machine. However, despite the advantages associated with the possible use of UHE ion beams for qualification of components to be used in the HE accelerator mixed-field environment, this paper shows that the associated volume-restricted LET values relevant for SEE characteristic SV sizes are not large enough (<15 MeVcm^2/mg) to guarantee the absence of silicon-dominated SEEs in their working environment.

Despite this limitation, the UHE beams in the CERN accelerator complex remain a very interesting option for SEE testing, both in terms of the practical advantages linked to the very high beam penetration, as well as research activities requiring such energies to mimic the possible impact of the GCR environment. Results of such research studies could have potential RHA implications related to the impact of energy on the ionization track structure or nuclear reactions.

References

[1] E. L. Petersen, V. Pouget, L. W. Massengill, S. P. Buchner, and D. McMorrow, "Rate predictions for single-event effects—Critique II," *IEEE Trans. Nucl. Sci.*, vol. 52, no. 6, pp. 2158–2167, Dec. 2005.

[2] R. G. Alía *et al.*, "Single event effects in high-energy accelerators," *Semicond. Sci. Technol.*, vol. 32, no. 3, p. 034003, Feb. 2017. [Online]. Available: http://stacks.iop.org/0268-1242/32/i=3/a=034003

[3] J. Mekki, M. Brugger, R. G. Alia, A. Thornton, N. C. Dos Santos Mota, and S. Danzeca, "CHARM: A mixed field facility at CERN for radiation tests in ground, atmospheric, space and accelerator representative environments," *IEEE Trans. Nucl. Sci.*, vol. 63, no. 4, pp. 2106–2114, Aug. 2016.

[4] R. G. Alía *et al.*, "LHC and HL-LHC: Present and future radiation environment in the high-luminosity collision points and RHA implications," *IEEE Trans. Nucl. Sci.*, vol. 65, no. 1, pp. 448–456, Jan. 2018.

[5] A. Virtanen, R. Harboe-Sørensen, H. Koivisto, S. Pirojenko, and K. Ranttila, "High penetration heavy ions at the RADEF test site," in *Proc. 7th Eur. Conf. Radiat. Effects Compon. Syst. (RADECS)*, Sep. 2003, pp. 499–502.

[6] A. Virtanen, R. Harboe-Sorensen, A. Javanainen, H. Kettunen, H. Koivisto, and I. Riihimaki, "Upgrades for the RADEF facility," in *Proc. IEEE Radiat. Effects Data Workshop*, Jul. 2007, pp. 38–41.

[7] B. D. Reddell *et al.*, "Compendium of single event effects test results for commercial-off-the-shelf and standard electronics for low earth orbit and deep space applications," in *Proc. IEEE Radiat. Effects Data Workshop (REDW)*, Jul. 2017, pp. 57–66.

[8] V. Ferlet-Cavrois *et al.*, "Influence of beam conditions and energy for SEE testing," *IEEE Trans. Nucl. Sci.*, vol. 59, no. 4, pp. 1149–1160, Aug. 2012.

[9] *Centre du Recherches du Cyclotron, Université Catholique de Louvain-la-Neuve*. Accessed: Sep. 2, 2018. Belgium, [Online]. Available: http://www.cyc.ucl.ac.be/

[10] *Radiation EFfects Facility—Accelerator Laboratory, University of Jyvaskyla*. Accessed: Sep. 2, 2018. [Online]. Available: https://www.jyu.fi/science/en/physics/research/infrastructures/accelerator-laboratory/radiation-effects-facility

[11] *Texas A&M University Cyclotron Institute Radiation Effects Facility*. Accessed: Sep. 2, 2018. [Online]. Available: http://cyclotron.tamu.edu/ref/

[12] *Berkeley Accelerator Space Effects—Lawrence Berkeley National Laboratory*. Accessed: Sep. 2, 2018. [Online]. Available: http://cyclotron.lbl.gov/base-rad-effects

[13] M.-H. Moscatello, A. Dubois, and X. Ledoux, "Industrial applications with GANIL SPIRAL2 facility," in *Proc. 16th Eur. Conf. Radiat. Effects Compon. Syst. (RADECS)*, Sep. 2016, pp. 1–3.

[14] *KVI—Center for Advanced Radiation Technology*. Accessed: Sep. 2, 2018. [Online]. Available: http://www.rug.nl/kvi-cart

[15] *NASA Space Radiation Laboratory at Brookhaven*. Accessed: Sep. 2, 2018. [Online]. Available: https://www.bnl.gov/nsrl/userguide/beam-ion-species-and-energies.php

[16] R. Koga, S. H. Crain, W. R. Crain, K. B. Crawford, and S. J. Hansel, "Comparative SEU sensitivities to relativistic heavy ions," *IEEE Trans. Nucl. Sci.*, vol. 45, no. 6, pp. 2475–2482, Dec. 1998.

[17] T. Böhlen *et al.*, "The FLUKA code: Developments and challenges for high energy and medical applications," *Nucl. Data Sheets*, vol. 120, pp. 211–214, Jun. 2014.

[18] G. Battistoni *et al.*, "Overview of the FLUKA code," *Ann. Nucl. Energy*, vol. 82, pp. 10–18, Aug. 2015.

[19] E. Mobs. (Aug. 2018). *The CERN Accelerator Complex*. Accessed: Sep. 2, 2018. [Online]. Available: https://cds.cern.ch/record/2636343

[20] R. G. Alía *et al.*, "SEE testing in the 24-GeV proton beam at the CHARM facility," *IEEE Trans. Nucl. Sci.*, vol. 65, no. 8, pp. 1750–1758, Aug. 2018.

[21] P. Fernandez-Martinez *et al.*, "SEE tests with ultra energetic Xe ion beam in the CHARM facility at CERN," in *Proc. 16th Eur. Conf. Radiat. Effects Compon. Syst. (RADECS)*, to be published.

[22] D. Manglunki *et al.* (2016). *CERN's Fixed Target Primary Ion Programme*. Accessed: Sep. 2, 2018. [Online]. Available: https://cds.cern.ch/record/2207350

[23] S. L. Weeden-Wright *et al.*, "Effects of energy-deposition variability on soft error rate prediction," *IEEE Trans. Nucl. Sci.*, vol. 62, no. 5, pp. 2181–2186, Oct. 2015.

[24] R. Ladbury, J.-M. Lauenstein, and K. P. Hayes, "Use of proton SEE data as a proxy for bounding heavy-ion SEE susceptibility," *IEEE Trans. Nucl. Sci.*, vol. 62, no. 6, pp. 2505–2510, Dec. 2015.

[25] R. G. Alía *et al.*, "Simplified SEE sensitivity screening for COTS components in space," *IEEE Trans. Nucl. Sci.*, vol. 64, no. 2, pp. 882–890, Feb. 2017. [Online]. Available: http://ieeexplore.ieee.org/document/7819485/

[26] K. A. Olive *et al.*, "Review of Particle Physics," *Chin. Phys.*, vol. C38, p. 090001, 2014. [Online]. Available: http://pdg.lbl.gov/2015/download/rpp2014-Chin.Phys.C.38.090001.pdf

[27] J. F. Ziegler, M. Ziegler, and J. Biersack, "SRIM—The stopping and range of ions in matter (2010)," *Nucl. Instrum. Methods Phys. Res. B, Beam Interact. Mater. At.*, vol. 268, nos. 11–12, pp. 1818–1823, Jun. 2010, [Online]. Available: http://www.sciencedirect.com/science/article/pii/S0168583X10001862

[28] G. Hubert, P. L. Cavoli, C. Federico, L. Artola, and J. Busto, "Effect of the radial ionization profile of proton on SEU sensitivity of nanoscale SRAMs," *IEEE Trans. Nucl. Sci.*, vol. 62, no. 6, pp. 2837–2845, Dec. 2015.

[29] M. P. King *et al.*, "Electron-induced single-event upsets in static random access memory," *IEEE Trans. Nucl. Sci.*, vol. 60, no. 6, pp. 4122–4129, Dec. 2013.

[30] S. Roesler, R. Engel, and J. Ranft, "The Monte Carlo event generator DPMJET-III," in *Advanced Monte Carlo for Radiation Physics, Particle Transport Simulation and Applications*, A. Kling, F. Barão, M. Nakagawa, L. Távora, and P. Vaz, Eds. Lisbon, Portugal: Springer, 2001, pp. 1033–1038. [Online]. Available: https://link.springer.com/content/pdf/10.1007%2F978-3-642-18211-2.pdf

[31] R. G. Alía *et al.*, "Sub-LET threshold SEE cross section dependency with ion energy," *IEEE Trans. Nucl. Sci.*, vol. 62, no. 6, pp. 2797–2806, Dec. 2015.

[32] R. G. Alía *et al.*, "Proton dominance of sub-LET threshold GCR SEE rate," *IEEE Trans. Nucl. Sci.*, vol. 64, no. 1, pp. 388–397, Jan. 2017.

[33] R. A. Reed *et al.*, "Impact of ion energy and species on single event effects analysis," *IEEE Trans. Nucl. Sci.*, vol. 54, no. 6, pp. 2312–2321, Dec. 2007.

[34] R. Harboe-Sorensen *et al.*, "From the reference SEU monitor to the technology demonstration module on-board PROBA-II," *IEEE Trans. Nucl. Sci.*, vol. 55, no. 6, pp. 3082–3087, Dec. 2008.

[35] R. Harboe-Sorensen *et al.*, "The technology demonstration module on-board PROBA-II," *IEEE Trans. Nucl. Sci.*, vol. 58, no. 3, pp. 1001–1007, Jun. 2011.

[36] R. Harboe-Sorensen *et al.*, "PROBA-II technology demonstration module in-flight data analysis," *IEEE Trans. Nucl. Sci.*, vol. 59, no. 4, pp. 1086–1091, Aug. 2012.

[37] S. Uznanski, B. Todd, A. Dinius, Q. King, and M. Brugger, "Radiation hardness assurance methodology of radiation tolerant power converter controls for large hadron collider," *IEEE Trans. Nucl. Sci.*, vol. 61, no. 6, pp. 3694–3700, Dec. 2014.

[38] W. Hajdas, F. Burri, C. Eggel, R. Harboe-Sorensen, and R. de Marino, "Radiation effects testing facilities in PSI during implementation of the Proscan project," in *Proc. IEEE Radiat. Effects Data Workshop*, Jul. 2002, pp. 160–164.